



## Relating the variability of tone-burst otoacoustic emission and auditory brainstem response latencies to the underlying cochlear mechanics

Sarah Verhulst and Christopher A. Shera

Citation: [AIP Conference Proceedings](#) **1703**, 090003 (2015); doi: 10.1063/1.4939401

View online: <http://dx.doi.org/10.1063/1.4939401>

View Table of Contents: <http://scitation.aip.org/content/aip/proceeding/aipcp/1703?ver=pdfcov>

Published by the [AIP Publishing](#)

---

### Articles you may be interested in

[Tone-burst auditory brainstem response wave V latencies in normal-hearing and hearing-impaired ears](#))

J. Acoust. Soc. Am. **138**, 3210 (2015); 10.1121/1.4935516

[Comparison of cochlear delay estimates using otoacoustic emissions and auditory brainstem responses](#)

J. Acoust. Soc. Am. **126**, 1291 (2009); 10.1121/1.3168508

[Tone-burst otoacoustic emissions and loudness](#)

J. Acoust. Soc. Am. **117**, 2454 (2005); 10.1121/1.4809378

[Latency of auditory brain-stem responses and otoacoustic emissions using tone-burst stimuli](#)

J. Acoust. Soc. Am. **83**, 652 (1988); 10.1121/1.396542

[Latency of otoacoustic emissions and ABR wave V using tone-burst stimuli](#)

J. Acoust. Soc. Am. **79**, S5 (1986); 10.1121/1.2023305

---

# Relating the Variability of Tone-Burst Otoacoustic Emission and Auditory Brainstem Response Latencies to the Underlying Cochlear Mechanics

Sarah Verhulst\* and Christopher A. Shera†

\*Cluster of Excellence Hearing4All and Medizinische Physik, Department of Medical Physics and Acoustics, University of Oldenburg, Oldenburg, Germany

†Eaton-Peabody Laboratories, Harvard Medical School, Boston, Massachusetts, USA

**Abstract.** Forward and reverse cochlear latency and its relation to the frequency tuning of the auditory filters can be assessed using tone bursts (TBs). Otoacoustic emissions (TBOAEs) estimate the cochlear roundtrip time, while auditory brainstem responses (ABRs) to the same stimuli aim at measuring the auditory filter buildup time. Latency ratios are generally close to two and controversy exists about the relationship of this ratio to cochlear mechanics. We explored why the two methods provide different estimates of filter buildup time, and ratios with large inter-subject variability, using a time-domain model for OAEs and ABRs. We compared latencies for twenty models, in which all parameters but the cochlear irregularities responsible for reflection-source OAEs were identical, and found that TBOAE latencies were much more variable than ABR latencies. Multiple reflection-sources generated within the evoking stimulus bandwidth were found to shape the TBOAE envelope and complicate the interpretation of TBOAE latency and TBOAE/ABR ratios in terms of auditory filter tuning.

## INTRODUCTION

Wave-V latency of auditory brainstem responses ( $\tau_{\text{ABR}}$ ) recorded to narrow-band tone-bursts have been used to derive the forward cochlear latency  $\tau_{\text{BM}}(x)$  in humans [4, 8, 10, 12].  $\tau_{\text{BM}}(x)$ , defined as the group delay of the basilar-membrane (BM) response at cochlear location  $x$ , appears related to the frequency tuning of the underlying auditory filter [15]. The cochlear roundtrip time  $\tau_{\text{OAE}}(f)$  can be derived using tone-burst OAE (TBOAE) latency [4, 8, 10, 12], and is defined as the time it takes a particular frequency component in the evoking stimulus to travel to the region where the emission is generated and back to the eardrum.

When emissions are generated through coherent reflection filtering occurring near the peak of the forward traveling wave, theoretical predictions map  $\tau_{\text{OAE}}$  to  $1.8\text{--}2\tau_{\text{BM}}$  [14]. A recent study measuring simultaneous ABR and OAEs to tone-bursts found ratios closer to 1 for stimulus frequencies (CFs) below 1.5 kHz and ratios above 2 for higher CFs [12]. These findings contradict earlier studies reporting ratios close to two (2 [8];  $2.08 \pm 0.19$  [5];  $1.92 \pm 0.42$  ms [4]). Reasons for these discrepancies are in part due to the methods adopted to separate the stimulus from the TBOAE onset.  $\tau_{\text{OAE}}$  suffers from an inter-subject variability as large as 10–30% [4, 10], a variability that is five times higher than for ABRs recorded in the same listeners [12].

The present study investigates the sources giving rise to inter-subject variations of the TBOAE and ABR latency methods using a modeling approach that is free from experimental TBOAE onset-separation errors. Implementations of a time-domain model for OAE and ABR generation were used to simulate ears from 20 listeners, in which all parameters but the random cochlear irregularities leading to coherent reflection-source OAEs were identical. The simulated TBOAE and ABR latency estimates aid in understanding why both methods can provide different estimates of auditory filter buildup time, leading to ratios that are not necessarily 1.8–2, even in a model based on emission generation through slow forward and reverse traveling waves.

## METHODS

A nonlinear time-domain model of the middle ear and cochlea that generates reflection- and distortion-source OAEs [16] was used as a preprocessor to an auditory-nerve (AN) model [19], after which a functional model for the ventral cochlear nucleus (VCN) and inferior colliculus (IC) was included [9]. Simulated ABR wave-I, III and V were obtained by summing the model responses across 500 simulated Greenwood spaced CFs at the level of the AN, CN and IC, respectively. To match the outputs of the cochlear model to the inputs of the AN model, several adjustments were

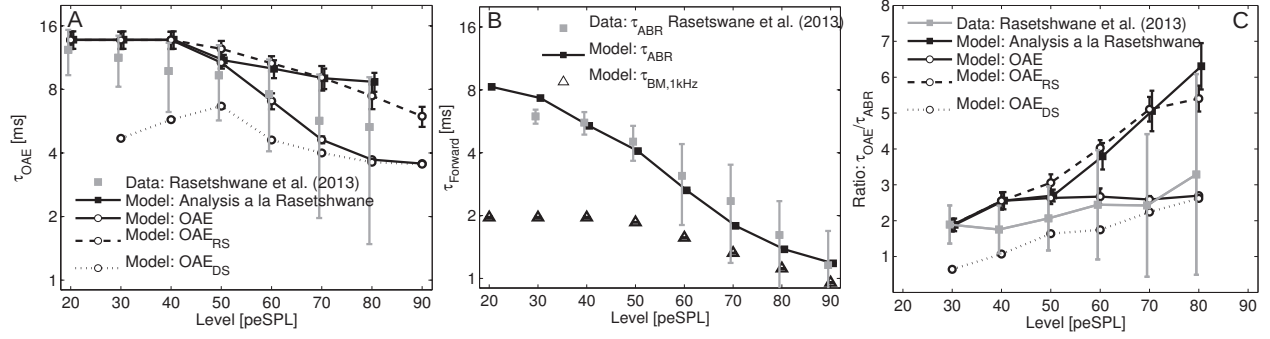


**FIGURE 1.** (A) Experimental and simulated  $\tau_{OAE}$  to 4-ms long 1-kHz tone bursts (no plateau), using the methods in [12] for 14 human subjects, and 20 frozen model subjects. Additionally,  $\tau_{OAE}$  calculated over the whole derived OAE, OAE<sub>RS</sub> and OAE<sub>DS</sub> waveforms are also shown. (B)  $\tau_{ABR}$  for the same stimuli and subjects as in panel A. Simulated  $\tau_{BM}$  calculated as the EWGD of the BM velocity response of the 1-kHz CF cochlear channel. (C) Experimental [12] and simulated  $\tau_{OAE}/\tau_{ABR}$  ratios. Ratios for OAE, OAE<sub>RS</sub>, OAE<sub>DS</sub> were calculated using the whole derived waveforms.

made to the existing AN model implementation [19]: (i) BM vibration was translated into inner-hair-cell (IHC) bundle deflection using a transformation gain constant, after which a 2<sup>nd</sup> order Boltzmann function and a 2<sup>nd</sup> order low-pass filter with cut-off frequency of 1 kHz were adopted to simulate the IHC receptor potential. (ii) AN fiber thresholds were made independent of CF, (iii) and made dependent on the spontaneous-rate (SR) of the fiber, and (iv), SR-dependence of the AN equations was modified to match the original implementation of the three-store diffusion model [17]. These adjustments lead to a 2-ms latency decrease in ABR wave-V latency for a 40-dB click level increase, a feature that is not accounted for in existing ABR models that only account for a  $\sim 0.5$  ms decrease [1, 13].

$\tau_{ABR}$  was calculated as the peak latency of the simulated ABR wave-V minus the synaptic delays introduced in the CN and IC model stages, comparable to the experimental ABR forward-latency method [12].  $\tau_{OAE}$  was calculated using the energy-weighted group delay (EWGD) [2, 12] of the OAE waveform in a window starting at a latency equal to the stimulus duration (4 ms) plus 0.5 ms, as in [12]. Simulated ear-canal pressure PEC consists of 3 components: STIM, representing the passive components of the response; and OAE<sub>RS</sub> and OAE<sub>DS</sub>, representing the reflection- and distortion-source OAE components. STIM was estimated by rescaling PEC computed in the low-level linear regime (20 dB SPL) using a model without micromechanical irregularities (i.e., no OAE<sub>RS</sub> and no OAE<sub>DS</sub>), leading to the  $OAE = OAE_{DS} + OAE_{RS} = PEC - STIM$ . OAE<sub>RS</sub> was obtained subtracting PEC from a model simulation where irregularities were first turned on, and then turned off:  $OAE_{RS} = PEC_{irr} - PEC_{no\ irr}$ . OAE<sub>DS</sub> can then readily be obtained using  $OAE_{DS} = OAE - OAE_{RS} = PEC_{no\ irr} - STIM$ . In addition to calculating the EWGD identically to the method used in [12], EWGDs were also calculated using the whole waveforms of the simulated OAE, OAE<sub>RS</sub> and OAE<sub>DS</sub>.  $\tau_{BM}$  was calculated from the EWGD of the simulated BM velocity waveform of the 1-kHz CF channel.

## RESULTS

To demonstrate that the model is suited to study TBOAE and ABR latency, Fig. 1 shows a direct comparison between the simulated TBOAE and ABR latencies and those obtained experimentally to 1-kHz TBs ( $t_{dur} = 4$  ms) of increasing intensity. When using the same latency method, simulated  $\tau_{ABR}$  fell within the bounds of the experimental standard deviations of the experimental study [12] for stimulus levels above 40 dB peSPL, demonstrating decreased ABR latencies for increased stimulus levels. Simulated  $\tau_{OAE}$  were found to match the experimental data well when calculating EWGDs over the whole derived waveform, but overestimate the latencies for stimulus levels above 60 dB peSPL when using the same analysis method employed in [12].

**Variability of latency estimates.** The standard deviations of the simulated  $\tau_{ABR}$  across 20 frozen model implementations were small compared to those found experimentally (Fig. 1B). Because the models were identical except for the micromechanical irregularities, experimental variability stemming from background noise and/or probe and electrode placement were not captured, and hence would not introduce variability in the simulated  $\tau_{ABR}$ . Because the variability was so small, we conclude that the ABR latency estimates were not affected by changes in the micromechanical irregularity patterns in the cochlea that were used to simulate different model subjects. The story is different when we evaluate the standard deviations of the simulated  $\tau_{OAE}$  in Fig. 1A. Even though our methods of deriving  $\tau_{OAE}$  are free

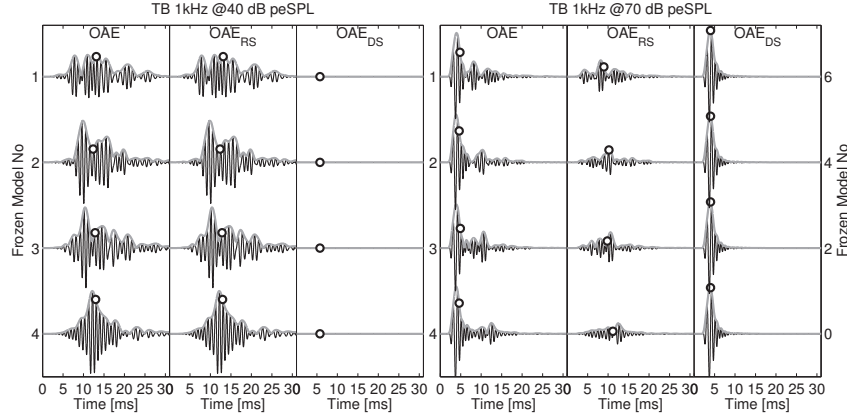


**FIGURE 2.** TBOAE waveforms and envelopes to 4-ms long 1-kHz tone bursts, simulated for 4 frozen model subjects and two stimulus levels. Derived OAE,  $OAE_{RS}$  and  $OAE_{DS}$  waveforms are shown and EWGDs are indicated by white markers.

from measurement noise, standard deviations up to 1.3 ms were found. Differences in experimental methods alone are thus not able to explain why five times larger standard deviations are found for  $\tau_{OAE}$  than for  $\tau_{BM}$  in the experimental data plotted [12]. The simulations in Fig. 1A and B indicate that differences in the generator mechanisms of both types of responses may explain the large variability in the latency estimates because the only difference in the frozen models implementation was the placement of the random irregularities on the BM giving rise to reflection-source OAEs.

Indeed, when plotting waveforms of the simulated TBOAEs for different model subjects (Fig. 2), it is clear that the envelopes of the waveforms show little similarity between subjects. The EWGD estimates (indicated by the white markers) are able to compensate for some of the variability in the waveform envelopes, but variation in  $\tau_{OAE}$  across frozen models is still apparent. For low stimulus levels, the  $OAE_{RS}$  component is responsible for the variations in waveform envelopes across subjects (left panel). For higher stimulation levels where a prominent  $OAE_{DS}$  component appears, the variations in  $\tau_{OAE}$  are smaller, because the variation on the latency of the dominating  $OAE_{DS}$  component is next to zero. Latencies  $\tau_{OAE}$  and standard deviations for the OAE,  $OAE_{RS}$ , and  $OAE_{DS}$  waveforms are summarized Fig. 1A. The variation in  $\tau_{OAE}$  is due to variations in the  $OAE_{RS}$  envelope, and becomes smaller at larger stimulation levels, for which the  $OAE_{DS}$  component dominates the response, and  $\tau_{OAE_{DS}}$  variations are absent.

**Reflection-source generators.** Variations in the simulated TBOAE<sub>RS</sub> envelopes arise through differences in the placement of the random irregularities along the BM. Thus, it is possible that emission components are generated at different cochlear locations, leading to different  $\tau_{OAE}(f)$  contributing to the total OAE. This idea was tested in a model that had one point-source BM irregularity ( $M_1$ ) placed at the cochlear location corresponding to the frequency of a peak of the simulated CEOAE spectrum. As a result, a relatively narrow band emission was generated in response to simulation with a click. A second point-source BM irregularity ( $M_2$ ), was added at a frequency corresponding to the nearest peak in the click-evoked OAE (CEOAE) spectrum of that model subject when all random irregularities were present.  $M_1$  and  $M_2$  thus investigate the influence of two distinct reflection-sources on the OAE waveform.

Figure 3 shows  $OAE_{RS}$  waveform envelopes and corresponding magnitude and phase spectra for different stimulus levels and three model versions with one or two point-sources present:  $M_1$ , and  $M_2$  alone, and both sources together  $M_{12}$ . Envelope maxima of the single source models decreased as stimulus level increased. This latency-decrease with level reflects group-delay changes of the forward traveling wave as observed from the fixed location of the reflector source (i.e., as judged from the shallower slopes of the phase patterns with level evaluated at the frequency corresponding to the source location  $M$ ). When two point-sources are present simultaneously, the relationship between latency and group delay becomes less apparent. At low stimulus levels, the  $OAE_{RS}$  envelope shows two bumps with neither maximum occurring at latencies corresponding to the maxima of the OAE envelopes in the single source models. As stimulus level increases, the first bump becomes more prominent than the second, with corresponding growth of the first bump more linear than that of the second (analysis not shown), in agreement with experimental filtered click CEOAE waveforms [3, 6, 11]. Additional analysis with TB stimuli and different source frequencies revealed that as long as the two sources were located within the stimulus bandwidth (i.e., 250 Hz for the 1-kHz TBs in this study), behavior qualitatively similar to that of

the double source waveform in Fig. 3 was obtained. Note that the mechanism giving rise to a latency of the first envelope bump shorter than that of either one of the point-source emissions ( $M_{12}$  vs  $M_1$  or  $M_2$ ) occurred here through beating of two emission components that travel out of the cochlea together. The exact phase and amplitude ratio between the emission components determines the envelope shape regardless of their exact relation to the center frequency of the stimulus. Waveform shapes and associated latencies did thus not need to arise from specific generators at more basal locations, as often referred to in other studies [7, 18]. The varying envelope shapes in Fig. 2 for different frozen model implementations, and associated variability in the  $\tau_{\text{OAE}}$  were in this model framework explained by beating between OAEs arising from multiple sources located within the peak region of the traveling wave.

**Latency ratios.** Because subject-dependent reflection-source emission generators shape the envelope of the TBOAEs causing variability on  $\tau_{\text{OAE}}$ , the ratios between  $\tau_{\text{OAE}}$  and  $\tau_{\text{ABR}}$  are also affected. As shown in Fig. 1, experimental ratios and those obtained using the whole simulated OAE waveform show ratios close to two for low stimulus levels, that increase towards 3 for higher stimulus levels. For the simulated results, the ratio is dominated by the latency of the reflection-source OAE component at low stimulus levels whereas it is dominated by the latency of the invariable distortion-source OAE component for the high levels. This also influences the variability of the ratio by showing larger variability for low stimulus levels. The experimental results do not show decreased variability of the ratio as stimulus level increases, which is likely due to the adopted windowing method that zero pads 4.5 ms of the recorded ear-canal-pressure to obtain the OAE waveform. Because for higher stimulus levels, the simulated  $\tau_{\text{OAE}_{\text{DS}}}$  was close to or shorter than 4.5 ms, it is possible that the experimental analysis was not able to include this emission component in  $\tau_{\text{OAE}}$  or the latency ratios.

**Relationship to  $\tau_{\text{BM}}$ .** The model approach allows for a direct comparison of simulated  $\tau_{\text{OAE}}$  and  $\tau_{\text{ABR}}$  to  $\tau_{\text{BM}}$ . Even though the model is able to capture the experimental forward-latency decrease with level derived from the ABR wave-V (Fig. 1B),  $\tau_{\text{ABR}}$  overestimates the model  $\tau_{\text{BM}}(1 \text{ kHz})$  derived from the simulated BM velocity waveform. For stimulus levels below 50 dB SPL the deviation is largest, whereas for high stimulus levels, the two waveforms run parallel. The deviation between the two measures arises because whereas  $\tau_{\text{BM}}(1 \text{ kHz})$  is a single channel estimate of filter build-up time,  $\tau_{\text{ABR}}$  is obtained from a population response shaped by excitation (and associated build-up times) along much of the BM. Comparison between  $\tau_{\text{BM}}(1 \text{ kHz})$  and  $\tau_{\text{OAE}}$  yields cochlear roundtrip times up to 8 times larger than  $\tau_{\text{BM}}(1 \text{ kHz})$  for  $\tau_{\text{OAE}_{\text{RS}}}$  and up to 3 times larger for  $\tau_{\text{OAE}_{\text{DS}}}$ . A quantitative comparison between latency estimates and ratios is limited by the overall quality of the model, and is not pursued at this stage. At this point, we conclude that even though our model simulates experimental data of 1-kHz TBOAE and ABRs well, neither the ratios nor the latency estimates derived from  $\tau_{\text{OAE}}$  and  $\tau_{\text{ABR}}$  capture well the underlying filter build-up time derived from  $\tau_{\text{BM}}(1 \text{ kHz})$ .

## DISCUSSION

$\tau_{\text{OAE}}$  and  $\tau_{\text{OAE}}/\tau_{\text{ABR}}$  ratios are affected by the reflection-source generator mechanisms giving rise to subject-dependent envelope shapes of the TBOAEs. This  $\tau_{\text{OAE}}$  variability, together with experimental difficulties in separating the stimulus from the TBOAE onset, imply that  $\tau_{\text{OAE}}$  and  $\tau_{\text{OAE}}/\tau_{\text{ABR}}$  are difficult to relate to auditory filter build-up time. The variability of  $\tau_{\text{OAE}}$  was due to the subject-dependent variations in the  $\text{OAE}_{\text{RS}}$  envelopes. Even though  $\text{OAE}_{\text{RS}}$  was generated through coherent reflection in the peak region of the traveling wave, the measure cannot easily be related to filter build-up time when multiple sources are present within the stimulus bandwidth. The double-bump behavior demonstrated here can account for the filtered click OAE data of [3], since the 1/3rd octave bandwidth adopted in that study allows for multiple CEOAE spectral peaks within the analysis window. Beating between multiple reflection sources within the evoking stimulus bandwidth can, even for TB stimuli, make it difficult to use this method to estimate individual filter build-up time. However, though the variability of the  $\tau_{\text{OAE}}$  method is much larger than that of the  $\tau_{\text{ABR}}$ , the  $\tau_{\text{OAE}}$  method has successfully demonstrated a frequency-dependence of auditory filter build-up time of the human

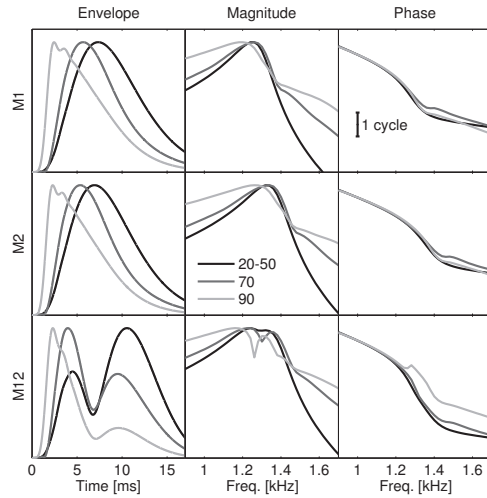


**FIGURE 3.** Envelopes and spectra for three point-source models stimulated with clicks (20–90 dB pe-SPL). Responses are normalized to their maximum amplitude.  $M_1$  and  $M_2$  represent single reflector sources at 1290 Hz and 1370 Hz; model  $M_{12}$  has both. Results are shown for the  $\text{OAE}_{\text{RS}}$  component.



auditory system, as calculated from the mean over a large body of subjects [4, 5, 8, 12].

$\tau_{\text{OAE}_{\text{DS}}}$  and  $\tau_{\text{ABR}}$  demonstrated little variability across frozen model implementation, and thus appear to be more robust measures. The relationship between  $\tau_{\text{ABR}}$  and the underlying single-channel filter build-up time remains unclear because  $\tau_{\text{ABR}}$  depends on simultaneous summing of energy across the excited channels. Though our simulations fell within bounds of experimental studies, the model may not accurately capture this cross-channel summation. In addition, we have not examined whether the current simulations correctly predict the relative amplitudes of the  $\text{OAE}_{\text{DS}}$  and  $\text{OAE}_{\text{RS}}$  components at higher stimulus levels. In the model, these relative amplitudes are determined by the form of the compressive nonlinearity and the roughness pattern, respectively. Simulated  $\tau_{\text{OAE}_{\text{DS}}}$  were closest to twice the modeled  $\tau_{\text{BM}}$  (1 kHz), and showed little variability across model subjects, making them a promising measure for cochlear roundtrip time. However, experimental demonstration of the  $\text{OAE}_{\text{DS}}$  response to TBs is difficult because of temporal overlap with the stimulus waveform. Nevertheless, it would be interesting to re-analyse existing data for evidence of this component and to test its relation to filter build-up times.

## ACKNOWLEDGMENTS

Supported by Oticon Foundation, DFG Cluster of Excellence Hearing4All, and NIH grant R01 DC003687.

## REFERENCES

- [1] Dau T (2003) The importance of cochlear processing for the formation of auditory brainstem and frequency following responses. *J Acoust Soc Am* 113:936–950
- [2] Goldstein JL, Baer T, Kiang NYS (1971) A theoretical treatment of latency, group delay, and tuning characteristics for auditory-nerve responses to clicks and tones. In: Sachs MB (ed) *Physiology of the Auditory System*, Baltimore: National Education Consultants, pp. 133–141
- [3] Goodman SS, Fitzpatrick DF, Ellison JC, Jesteadt W, Keefe DH (2009) High-frequency click-evoked otoacoustic emissions and behavioral thresholds in humans. *J Acoust Soc Am* 125:1014–1032
- [4] Harte JM, Pigasse G, Dau T (2009) Comparison of cochlear delay estimates using otoacoustic emissions and auditory brainstem responses. *J Acoust Soc Am* 126:1291–1301
- [5] Moleti A, Sisto R (2008) Comparison between otoacoustic and auditory brainstem response latencies supports slow backward propagation of otoacoustic emissions. *J Acoust Soc Am* 123:1495–1503
- [6] Moleti A, Botti T, Sisto R (2012) Transient-evoked otoacoustic emission generators in a nonlinear cochlea. *J Acoust Soc Am* 131:2891–2903
- [7] Moleti A, Al-Maamury AM, Bertaccini D, Botti T, Sisto R (2013) Generation place of the long- and short-latency components of transient-evoked otoacoustic emissions in a nonlinear cochlear model. *J Acoust Soc Am* 133:4098–4108
- [8] Neely ST, Norton SJ, Gorga MP, Jesteadt W (1988) Latency of auditory brain-stem responses and otoacoustic emissions using tone-burst stimuli. *J Acoust Soc Am* 83:652–656
- [9] Nelson PC, Carney LH (2004) A phenomenological model of peripheral and central neural responses to amplitude-modulated tones. *J Acoust Soc Am* 116:2173–2186
- [10] Norton SJ, Neely ST (1987) Tone-burst-evoked otoacoustic emissions from normal-hearing subjects. *J Acoust Soc Am* 81:1860–1871
- [11] Rasetshwane DM, Neely ST (2012) Measurements of wide-band cochlear reflectance in humans. *J Assoc Res Otolaryngol* 13:591–607
- [12] Rasetshwane DM, Argenyi M, Neely ST, Kopun JG, Gorga MP (2013) Latency of tone-burst-evoked auditory brainstem responses and otoacoustic emissions: level, frequency, and rise-time effects. *J Acoust Soc Am* 133:2803–2817
- [13] Rønne FM, Dau T, Harte JM, Elberling CE (2012) Modeling auditory evoked brainstem responses to transient stimuli. *J Acoust Soc Am* 131:3903–3913
- [14] Shera CA, Tubis A, Talmadge CL (2010) Testing coherent reflection in chinchilla: auditory-nerve responses predict stimulus-frequency emissions. *J Acoust Soc Am* 124:381–395
- [15] Shera CA, Guinan JJ Jr, Oxenham AJ (2010) Otoacoustic estimation of cochlear tuning: validation in the chinchilla. *J Assoc Res Otolaryngol* 11:343–365
- [16] Verhulst S, Dau T, Shera CA (2012) Nonlinear time-domain cochlear model for transient stimulation and human otoacoustic emission. *J Acoust Soc Am* 132:3842–3848
- [17] Westerman LA, Smith RL (1988) A diffusion model of the transient response of the cochlear inner hair cell synapse. *J Acoust Soc Am* 83:2266–2276
- [18] Withnell RH, Hazlewood C, Knowlton A (2008) Reconciling the origin of the transient evoked otoacoustic emission in humans. *J Acoust Soc Am* 123:212–221
- [19] Zilany MSA, Bruce IC, Nelson PC, Carney LH (2009) A phenomenological model of the synapse between the inner hair cell and auditory nerve: long-term adaptation with power-law dynamics. *J Acoust Soc Am* 126:239–2412

## COMMENTS AND DISCUSSION

**Alessandro Altoè:** Hello! Interesting study, with clear conclusions. I have just a concern: from your conclusions it seems that the latency of OAE might be a good measure of  $T_{bm}$  if it wasn't for OAEs which add a lot of randomness to the latency estimates. It looks to me that the "biggest" limitation of these estimates is the method used to compute the latency. In fact, the spectral components of OAEs have different group delay and magnitude that depend on the cochlear irregularities. So, the energy-weighted group delay (the center of gravity) might not give a very reliable measure of latency in this case (e.g. if the spectral region containing the most energy is the one which is the most delayed, then the latency is going to be largely overestimated). Computing the TBOAE latency with a threshold function or other methods might significantly reduce the variance of the estimated latency.

**Sarah Verhulst [reply to Alessandro Altoè]:** Dear Alessandro, thank you for your comment.  $T_{bm}$  can be reliably estimated from OAE<sub>rs</sub> when there is only one reflection source along the cochlear partition contributing to the response (Fig 3, top two panels). In that case, the EWGD will reflect the tuning of the underlying filter. In reality, multiple reflection sources are present, whose relative amplitudes and phase delays will affect the OAE<sub>rs</sub> envelope shape. Estimating latency from this multi-source OAE<sub>rs</sub> does not reflect the underlying filter latency, no matter which method you adopt. The EWGD is incorrect, but so would a threshold estimate, or one based on the latency of the first peak of the TBOAE (as other studies apply). All the above estimates will show variability in the  $T_{bm}$  estimate across listeners because of how multiple reflection sources generated through coherent reflection filtering within the evoking bandwidth on the BM interact and shape the resulting OAE<sub>rs</sub> envelope. Regards, Sarah.